DELPHI 99-12 CONF 212
5 February, 1999

Search for Stop and Sbottom at $\sqrt{s} = 130$ to 189 GeV

W. Da Silva, F. Kapusta, A. Savoy Navarro
LPNHE, University of Paris VI & VII, Paris, France

M. Besançon, Ph. Gris
CEA/DAPNIA/SPP, Saclay, France

Abstract

Data taken by the DELPHI experiment at a centre-of-mass energy of 189 GeV have been used to search for the supersymmetric partners of the top and bottom quark. The observations are in agreement with standard model predictions. These results are subsequently combined with those obtained by DELPHI during the 1995, 1996 and 1997 LEP runs and are interpreted in terms of exclusion regions in the ($M_{\tilde{q}}$, $M_{\tilde{\chi}_1^0}$) planes.

1 Introduction

This paper reports on a search for scalar partners of quarks (squarks) in data taken by DELPHI in 1998 at a centre-of-mass energy, $\sqrt{s}$, of 189 GeV. Mass limits for these particles have already been published based on data taken at LEP2 [1], [2], [5].

Scalar partners of right- and left-handed fermions are predicted by supersymmetric models and, in particular, by the minimal supersymmetric extension of the standard model (MSSM) [3]. They could be produced pairwise via e^+e^- annihilation into Z^0/γ. Important effects caused by off-diagonal terms in the mass matrix are only predicted for the partners of heavy fermions.

As a consequence their lighter states are candidates for the lightest charged supersymmetric particle.

Throughout this paper conservation of R-parity is assumed, which implies that the lightest supersymmetric particle (LSP) is stable. In this paper the LSP is assumed to be the lightest neutralino which only weakly interacts with normal matter, such that events will be characterised by missing momentum and energy.

In a large fraction of MSSM parameter space sfermions are supposed to decay dominantly into the corresponding fermion and the lightest neutralino. Consequently for sbottom only the decay into $b + \tilde{\chi}_1^o$ was considered in this paper. For the stop squark, the equivalent decay into $t + \tilde{\chi}_1^o$ is kinematically not allowed, and a stop decay into a bottom quark and a chargino is disfavoured in view of existing limits on the chargino mass [4]. The dominant two-body decay channel is thus the one into a charm quark and a neutralino. More details on squark phenomenology can be found in [7].

2 Detector description

The DELPHI detector and its performance have been described in detail elsewhere [8, 9]; only those components relevant for the present analyses are discussed here. Charged particle tracks are reconstructed in the 1.2 T solenoidal magnetic field by a system of cylindrical tracking chambers. These are the Microvertex Detector (VD), the Inner Detector (ID), the Time Projection Chamber (TPC) and the Outer Detector (OD). In addition, two planes of drift chambers aligned perpendicular to the beam axis (Forward Chambers A and B) track particles in the forward and backward directions, covering polar angles $11^\circ < \theta < 33^\circ$ and $147^\circ < \theta < 169^\circ$ with respect to the beam (z) direction.

The VD consists of three cylindrical layers of silicon detectors, at radii 6.3 cm, 9.0 cm and 11.0 cm. All three layers measure coordinates in the plane transverse to the beam. The closest (6.3 cm) and the outer (11.0 cm) layers contained double-sided detectors to also measure z coordinates. The VD covers polar angles from 24° to 156° and detectors have been added to the inner layer providing a measurement of the z coordinate. The ID consists of a cylindrical drift chamber (inner radius 12 cm and outer radius 22 cm) covering polar angles between 15° and 165°. The TPC, the principal tracking device of DELPHI, consists of a cylinder of 30 cm inner radius, 122 cm outer radius and had a length of 2.7 m. Each end-plate has been divided into 6 sectors, with 192 sense wires used for the dE/dx measurement and 16 circular pad rows used for 3 dimensional space-point reconstruction. The OD consists of 5 layers of drift cells at radii between 192 cm and 208 cm, covering polar angles between 43° and 137°.

The average momentum resolution for the charged particles in hadronic final states are in the range $\Delta p/p^2 \simeq 0.001$ to $0.01(\mathrm{GeV}/c)^{-1}$, depending on which detectors are used in the track fit [9].

The electromagnetic calorimeters consist of the High density Projection Chamber (HPC) covering the barrel region of $40^\circ < \theta < 140^\circ$, the Forward ElectroMagnetic Calorimeter (FEMC) covering $11^\circ < \theta < 36^\circ$ and $144^\circ < \theta < 169^\circ$, and the STIC, a Scintillator TIle Calorimeter which extends the coverage down to 1.66° from the beam axis in both directions. The 40° taggers are made of single layer scintillator-lead counters used to veto electromagnetic particles that may be not measured in the region between the HPC and FEMC. The efficiency to register a photon with energy above 5 GeV at polar angles between 20° and 160°, measured with the LEP1 data, is greater 99% [10]. The hadron calorimeter (HCAL) covers 98% of the solid angle. Muons with momenta above 2 GeV/c penetrates the HCAL and are recorded in a set of Muon Drift Chambers.

Decays of b-quarks are tagged using a probabilistic method based on the impact parameters of tracks with respect to the main vertex. The quantity $\mathcal{P}_E$ stands the probability that all tracks are compatible with the main vertex. $\mathcal{P}_E^+$ stands for the corresponding probability for tracks with positive impact parameters, the sign of the impact parameter being defined by the jet direction. The combined probability $\mathcal{P}_{comb}$ includes in addition contributions from properties of reconstructed secondary vertices [11].

3 Data samples, event generators and limits

Data have been taken during the 1998 LEP run at a mean centre-of-mass energy of 189 GeV, corresponding to an integrated luminosity of 158 pb^{-1}.

Simulated events are generated with several different programs in order to evaluate signal efficiency and background contamination. All the models use `JETSET` 7.4 [12] for quark fragmentation with parameters tuned to represent DELPHI data [13].

Stop events are generated according to the expected differential cross-sections, using the `BASES` and `SPRING` program packages [15]. Special care has been taken in the modelling of the stop hadronisation [16]. Sbottom events are generated with the `SUSYGEN` program [14]. The background processes $\mathrm{e^+e^-} \to \mathrm{q\bar{q}}(n\gamma)$ and processes leading to four-fermion final states, $(\mathrm{Z}^0/\gamma)^*(\mathrm{Z}^0/\gamma)^*$, $\mathrm{W}^{+*}\mathrm{W}^{-*}$, $\mathrm{We}\nu_\mathrm{e}$, and $\mathrm{Z}^0\mathrm{e}^+\mathrm{e}^-$ were generated using `PYTHIA` [12]. The cut on the invariant mass of the virtual $(\mathrm{Z}^0/\gamma)^*$ in the $(\mathrm{Z}^0/\gamma)^*(\mathrm{Z}^0/\gamma)^*$ process has been set at 2 GeV/c^2, in order to determine the background from low mass $\mathrm{f\bar{f}}$ pairs. The calculation of the four-fermion background has been cross-checked using the program `EXCALIBUR` [17], which consistently takes into account all amplitudes leading to a given four-fermion final state. The version of `EXCALIBUR` used does not, however, include the transverse momentum of initial state radiation. Two-photon interactions leading to hadronic final states have been simulated using `TWOGAM` [18] and `BDKRC` [19] for the Quark Parton Model contribution. Leptonic final states with muons and taus are also modelled with `BDKRC`. `BDK` [19] is used for final states with electrons only.

Generated signal and background events is passed through detailed detector response simulation [20] and processed with the same reconstruction and analysis programs as the real data. The number of background events simulated is mostly several times larger than the number expected in the real data.

4 Event selection

In this section a search for stop and sbottom in the decay modes $c\tilde{\chi}_1^0$ and $b\tilde{\chi}_1^0$, respectively, is presented. In both cases the experimental signatures consist of events with two jets and missing momentum. Since event parameters, such as visible energy, depend highly on the mass difference ΔM between squark and LSP, optimised selection procedures are used for the degenerate ($\Delta M \leq 10\,\mathrm{GeV}/c^2$), and the non-degenerate ($\Delta M > 10\,\mathrm{GeV}/c^2$) mass case. The main differences between stop and sbottom events arise from the hadronisation, which occurs either before ($\tilde{\mathrm{t}}$) or after ($\tilde{\mathrm{b}}$) the decay of the scalar quark. These differences are visible in particular in the degenerate mass case. Consequently different selections are used for the stop and sbottom analyses in the degenerate mass case whereas the selections are identical in the non-degenerate mass case. The present analysis of the data taken at a mean centre-of-mass energy of 189 GeV follows the lines of the analysis of the data taken at a mean centre-of-mass energy of 183 GeV described in [6].

In a first step particles are selected and clustered into jets using the Durham algorithm with the critical distance set to 0.08. Reconstructed charged particles are required to have momenta above 100 MeV/c and impact parameters below 4 cm in the transverse plane and below 10 cm in the beam direction. Clusters in the calorimeters are interpreted as neutral particles if they are not associated to charged particles, and if their energy exceeds 100 MeV.

In the second step of the analysis, hadronic events are selected. Only two-jet events are accepted. The following requirements are optimised separately for the two ΔM regions:

Non-degenerate mass case: For both the stop and sbottom analysis hadronic events are selected by requiring at least eight charged particles, a total transverse energy greater than 15 GeV and a transverse energy of the most energetic jet greater than 10 GeV. These three cuts are also aimed at reducing the background coming from two-photon processes. Forward Bhabha scattering is suppressed by requiring that the total energy in the FEMC is lower than 25 GeV. $\mathrm{Z}(\gamma)$ processes with a detected photon are reduced by requiring that the total energy in the HPC is lower than 40 GeV. Finally, the polar angles of the two jets are required to be in the interval $[20^\circ, 160^\circ]$.

Degenerate mass case: For the selection of hadronic events for the stop analysis the number of charged particles is required to be greater than five, the total charged energy has to be lower than $0.3\sqrt{s}$ in order to select events with missing energy and the polar angle of the total missing momentum has to be in the interval $[15^\circ, 165^\circ]$, off the forward region, in order to reduce the background from radiative return events. The total energy in the FEMC and HPC has to be lower than 10 GeV and 40 GeV, respectively. The reduction of two-photon processes is ensured by requiring that the total transverse energy is greater than 5 GeV and that the quantity $p_{tt} = \sqrt{p_{tt1}^2 + p_{tt2}^2}$ is greater than 5 GeV, where p_{tti} is the transverse momentum of jet i with respect to the thrust axis in the transverse plane. Finally, the most energetic charged particle is required to have a polar angle in the interval $[30^\circ, 150^\circ]$ and a momentum greater than 2 GeV/c. Similarly the polar angle of the most energetic neutral particle is required to be in the interval $[20^\circ, 160^\circ]$. The sbottom selection at this step is similar to the stop analysis described above where only the requirement on the quantity p_{tt} has been removed.

After this second step and for both the non-degenerate and the degenerate mass cases, agreement between data and expectations from Monte Carlo describing standard model processes is found to be good as can be seen from Figures 1a-c showing the visible mass, the charged multiplicity and the fraction of the energy in the polar angle interval $[30^o, 150^o]$. Figures 2a-b show the total energy and the transverse energy, and Figure 2d shows the charged multiplicity of the leading jet, these for the degenerate mass case of the stop analysis. Figures 3a-c show the visible mass, the missing transverse energy and the total multiplicity. Finally, Figure 1d shows the discriminating function against the $Z\gamma$ background for the non degenerate mass case, Figure 2c and 3d show the discriminating functions for the degenerate mass domains of the stop and sbottom analyses. For these degenerate mass cases, fair agreements between data and expectations from Monte Carlo describing standard model processes are found.

In a third step discriminating linear functions [21] are used in order to achieve optimum rejection power. The composition of the functions is shown in Table 1. They have been determined in the following way:

Non-degenerate mass case: In this case, the same functions have been used both for the stop and the sbottom analysis. A first discriminating linear function has been determined using training samples of signal and Z(γ) background processes. For the training of a second discriminating linear function signal and WW background event samples have been used. In the non-degenerate mass case, these two sources of background processes are found to be dominant after the first and second step of the event selection.

Degenerate mass case: Here the main source of background remaining after the first and second step of the event selection is found to be $\gamma\gamma$ events. Different functions have been determined for the stop and sbottom analyses using training samples of signal and two-photon events.

The final background reduction is performed by sequential cuts. In the non-degenerate mass case, one set of cuts is used to select both stop and sbottom events. It is shown, together with the number of events retained in data and background simulation, in Table 2. The ratio of the total energy in a cone of 30° off the beam-axis to the total energy has to be bigger than 0.8, the ratio of the total energy in a cone of 20° off the beam-axis to the total energy has to be bigger than 0.95, the energy of the charged particle and the energy of the leading neutral particle have to be lower than 25 GeV and the ratio of the total electromagnetic energy of the next leading jet to the total energy of this next leading jet has to be lower than 0.2. As for the sbottom analysis an additional requirement concerns a cut on the combined b-tagging probability.

In the degenerate mass case two different selections are used for stop and sbottom, shown in Tables 3 and 4. The product of the fraction of the total energy in a cone of 30° off the beam-axis with the total transverse energy has to be greater than 1, the quantity p_{tt} defined above has to be greater than 4 GeV, the cosine of the acoplanarity angle with respect to the thrust axis has to be greater than -0.98 and finally the last requirement concerns the combined b-tagging probability.

5 Results

The number of candidates found and the expected background levels are shown in Table 5. One candidate event from the non-degenerate mass case analysis is shown in Figure 4. The efficiencies of the stop and sbottom signal selection are summarised in Figure 5. They have been evaluated using 35 simulated samples at different points in the ($M_{\tilde{q}}$,$M_{\tilde{\chi}^0_1}$) plane, for squark masses between 50 and 90 GeV/c^2 and neutralino masses between 0 and 85 GeV/c^2.

No evidence for stop or sbottom production has been found in the two-body decay channels. Figure 6 and Figure 7 show the ($M_{\tilde{q}}$,$M_{\tilde{\chi}^0_1}$) regions excluded at 95% confidence level by the search for $\tilde{t} \to c\tilde{\chi}^0_1$ and $\tilde{b} \to b\tilde{\chi}^0_1$ decays, with the 100% branching ratio assumption, both for purely left-handed states and the states with minimum cross section. We have also used the results of the analyses of the data at 130-183 GeV in order to derive these exclusion regions.

6 Conclusions

In a data sample of 158 pb^{-1} collected by the DELPHI detector at a centre-of-mass energy of 189 GeV searches are performed for events with acoplanar jet pairs. The results are combined with those already obtained at centre-of-mass energies between 130–183 GeV .

The search for stop and sbottom quarks, decaying into $c\tilde{\chi}^0_1$ and $b\tilde{\chi}^0_1$, respectively, gives in total 9 candidates well compatible with the expected background [1] of 11.6 ± 1.4.

For the stop, a mass limit of 79 GeV/c^2 is obtained for the state with minimal cross-section, if the mass difference between the squark and the LSP is above 15 GeV/c^2 . A mass limit of 62 GeV/c^2 is obtained for the sbottom quark under the same condition.

In the case of maximum cross-section, these numbers are 84 GeV/c^2 for the stop and 87 GeV/c^2 for the sbottom.

These results extend substantially exclusion limits obtained at LEP1 and at LEP2 centre-of-mass energies between 130–183 GeV.

Acknowledgements

We express our gratitude to the members of the CERN accelerator divisions and compliment them on the fast and efficient commissioning and operation of the LEP accelerator in this new energy regime.

[1] There are candidates in common in both the stop and sbottom analyses and the total background is given assuming a "or" of both stop and sbottom analyses. The numbers for the stop analysis and the sbottom analysis individually are given in table 5.

References

[1] DELPHI Collaboration: P. Abreu *et al.*, *Search for Scalar Fermions and Long-Lived Scalar Leptons at Centre-of-mass Energies of 130* GeV *to 172* GeV, submitted to E. Phys. J. C.

[2] ALEPH Collaboration: R. Barate *et al.*, *Search for sleptons in* e^+e^- *collisions at centre-of-mass energies up to 184 GeV*, CERN EP/98-077;
ALEPH Collaboration: R. Barate *et al.*, *Scalar quark searches at* $\sqrt{s}$ *= 181 – 184 GeV*, CERN EP/98-076;
L3 Collaboration: M. Acciarri *et al.*, *Search for Scalar Leptons, Charginos and Neutralinos in* e^+e^- *collisions at* $\sqrt{s}$ *= 161 – 172* GeV, CERN PPE/97-130, acc. by. E. Phys. J. C;
OPAL Collaboration: K. Ackerstaff *et al.*, Phys. Lett. **B396** (1997) 301;
OPAL Collaboration: K. Ackerstaff *et al.*, Z. Phys. **C75** (1997) 409.

[3] P. Fayet and S. Ferrara, Phys. Rep. **32** (1977) 249;
H.P. Nilles, Phys. Rep. **110** (1984) 1;
H.E. Haber and G. L.Kane, Phys. Rep. **117** (1985) 75.

[4] ALEPH Collaboration: R. Barate *et al.*, E. Phys. J. **C2** (1998) 417;
DELPHI Collaboration: P. Abreu *et al.*, E. Phys. J. **C1** (1998) 1;
L3 Collaboration: M. Acciarri *et al.*, op. cit., CERN PPE/97-130;
OPAL Collaboration: K. Ackerstaff *et al.*, E. Phys. J. **C2** (1998) 213.

[5] M. Besançon, Ph. Gris, *Stop and Sbottom Searches with DELPHI at LEP running at* $\sqrt{s}$*= 133 GeV and* $\sqrt{s}$*= 136 GeV*, DELPHI 96-25 PHYS 600;
Ph. Gris,*Stop and sbottom searches at* $\sqrt{s}$ *=161 and 172 GeV*, DELPHI 97-175 PHYS 749;
W. Adam, P. Allport, S. Amato, M. Berggren, M. Besançon, A. Galloni, M. Gandelman, Ph. Gris, B. King, J. H. Lopes, R. Pain and Ph.Schwemling, *Search for Sfermions at* $\sqrt{s}$ *= 183 GeV*, 98-57 MORIO CONF 130.

[6] W. Adam, P. Allport, S. Amato, M. Berggren, M. Besançon, A. Galloni, M. Gandelmann, Ph. Gris, B. King, J. H. Lopes, N. Neumeister, R. Pain and Ph. Schwemling, *Search for Sfermions at* $\sqrt{s}$ *= 130 to 183 GeV*, DELPHI 98-92 ICHEP'98 CONF 160.

[7] Ph. Gris, "*Phénoménologie et recherche de squarks à LEP200 avec le détecteur DELPHI*", Ph.D.thesis, DAPNIA-SPP 98-1001, Université Paris VI;
Ph. Gris, *On Sbottom hadronization at LEP200*, DELPHI 97-4 PHYS 663;
Ph. Gris, *On squarks searches in the light gravitino scenario*, DELPHI 97-175 PHYS 749.

[8] DELPHI Collaboration: P. Abreu *et al.*, Nucl. Instr. and Meth. **A303** (1991) 233.

[9] DELPHI Collaboration: P. Abreu *et al.*, Nucl. Instr. and Meth. **A378** (1996) 57.

[10] P. Rebecchi, "*Optimisation de l'herméticité du détecteur DELPHI pour la recherche de particules supersymétriques à LEP2* ", Ph.D.thesis, LAL 96-30, Université Paris XI Orsay.

[11] G. Borisov, C. Mariotti, *Performance of b-tagging in DELPHI at LEP2*, DAPNIA/Spp Report 97-06 and INFN/ISS Report 97-03;
G. Borisov, *Combined b-tagging*, DELPHI 97-94 PHYS 716,

[12] T. Sjöstrand, Comp. Phys. Comm. **82** (1994) 74;
T. Sjöstrand, "*High energy physics event generation with* `PYTHIA 5.7` *and* `JETSET 7.4`", CERN TH/7111-93 (1993, rev. 1994).

[13] DELPHI Collaboration: P. Abreu *et al.*, Z. Phys. **C73** (1996) 11.

[14] S.Katsanevas and S.Melachroinos in *Physics at LEP2*, CERN 96-01, Vol.2, p.328.

[15] S. Kawabata, Comp. Phys. Comm. **41** (1986) 127.

[16] W. Beenakker, R. Hopker, M. Spira, and P.M. Zerwas, Phys. Lett. **B349** (1995) 463.

[17] F.A. Berends, R. Pittau, R. Kleiss, Comp. Phys. Comm. **85** (1995) 437.

[18] S. Nova, A. Olshevski, and T. Todorov, "*A Monte Carlo event generator for two photon physics*", DELPHI note 90-35 PROG 152.

[19] F.A. Berends, P.H. Daverveldt, R. Kleiss, Monte Carlo Simulation of Two-Photon Processes, Comp. Phys. Comm. 40 (86) 271-284.

[20] `DELSIM` *Reference Manual*, DELPHI note 87-97 PROG 100.

[21] R.A. Fisher, *The use of multiple measurements in taxonomic problems*, Annals of Eugenics, **7** (1936).

[22] OPAL Collaboration: R. Akers *et al.*, Phys. Lett. **B337** (1994) 207.

[23] CDF Collaboration: *Search for Scalar Top*, abstract 652 submitted to ICHEP98.

	$\Delta M > 10\,\mathrm{GeV}/c^2$		$\Delta M \leq 10\,\mathrm{GeV}/c^2$	
	1st DLA	2nd DLA	DLA ($\tilde{\mathrm{t}}$)	DLA ($\tilde{\mathrm{b}}$)
Constant	2.248	3.855	1.701	-2.375
E_{vis}	-	-	-0.167	0.453
E_{30}	-0.364	-	-	3.411
E^{ch}	-	-	-0.085	-
E (jet 1)	-0.049	-	-	-0.544
E (jet 2)	-	0.059	-	-0.594
E^{ch} (jet 1)	-	-	0.193	-
E_T (jet 1)	0.047	-	-	-
E_T (jet 2)	-	-	0.135	-
E_T^{ch} (jet 1)	-	-	-	-0.17
P_T^{miss}	-	-	0.203	0.069
M_{vis}	-	-0.063	-	-
H_2	-	3.213	-	-
$\cos(acop)$	-	-	1.019	-
$\mathcal{P}_E^+$	-	-0.668	-0.672	-
$\mathcal{P}_{comb}$	-	-	-	0.692
θ_{iso}^{ch}	-	-0.013	-	-
$\cos(acop)$	1.605	-	-	-
$thrust$	-	-4.223	-	-
N^{ch}	-	-	-	0.248
$\lvert\cos(\theta_{thr})\rvert$	-	-	-0.797	-

Table 1: Coefficients of the discriminating linear functions (DLA) used in the second step of the search for two-body decays of stop and sbottom. For the non-degenerate mass case the first and second functions applied to both the $\tilde{\mathrm{t}}$ and $\tilde{\mathrm{b}}$ selections (see text). Jets are ordered according to their energy. E_{vis} denotes the visible energy, E_{30} the energy in the polar angle interval $[30^\circ, 150^\circ]$, p_T^{miss} the missing transverse momentum, M_{vis} the visible mass and H_i the i^{th} Fox-Wolfram moment. The superscript "ch" indicates use of charged tracks only, N^{ch} being the charged multiplicity and the subscript "T" quantities calculated in the transverse plane. $\mathcal{P}_E^+$ and $\mathcal{P}_{comb}$ are b-tagging probabilities as explained in the text. Finally, θ_{iso}^{ch} is the isolation angle of the most isolated charged particle, and θ_{thr} the polar angle of the thrust axis .

Selection	$\tilde{t}$ and $\tilde{b}$: $\Delta M > 10\,\mathrm{GeV}/c^2$	
	Data	MC
1st and 2nd step	6507	6659 ± 12
3rd step (DLA1)	130	125 ± 3
3rd step (DLA2)	22	24 ± 2
$E_{30} > 0.80$	15	12.9 ± 1.1
$E_{20} > 0.95$	12	11 ± 0.9
$P^{leading} < 25$ GeV	7	7.6 ± 0.9
$E_{em2}/E(jet2) \leq 0.2$	5	7 ± 0.9
$\mathcal{P}_{comb} \geq$-1 for $\tilde{b}$: only	2	2.2 ± 0.4

Table 2: Fourth step of the event selection for two-body decays of stop and sbottom in the non-degenerate mass case. DLA1 and DLA2 denote the first and second discriminating linear analysis as explained in the text. E_{30} (E_{20}) denotes the fraction of the total energy for the polar angles $> 30°$ and $150° >$ ($> 20°$ and $160° >$) from the beam axis respectively. $P^{leading}$ denotes the momentum of the leading particle E_{em2} denotes the total electromagnetic energy of the next to leading jet. $\mathcal{P}_{comb}$ is a b-tagging probability as explained in the text.

Selection	$\tilde{t}$: $\Delta M \leq 10\,\mathrm{GeV}/c^2$	
	Data	MC
1st and 2nd step	1613	1567±45
3rd step (DLA)	139	134±10
oblateness $\geq$0.1	115	106±5
$E_{30} \geq 0.9$	76	79±4
$E_{20} \geq 0.985$	65	68±4
$P_{tt} \leq 30\,\mathrm{GeV}/c$	29	40±4
$\phi^{thr}_{acop} \geq 20°$	8	8.1±1.6
$\cos(acop) \geq -0.85$	3	3.3±0.8

Table 3: Fourth step of the event selection for two-body decays of stop squarks in the degenerate mass case. E_{30} (E_{20}) denotes the fraction of the total energy for the polar angles $> 30°$ and $150° >$ ($> 20°$ and $160° >$) from the beam axis respectively. For the other variables see the text and Table 1. DLA stands for discriminating linear analysis.

Selection	$\tilde{\mathrm{b}}$: $\Delta M \leq 10\,\mathrm{GeV}/c^2$	
	Data	MC
1^{st} and 2^{nd} step	5307	5644±106
3^{rd} step (DLA)	19	26±7
$E_{20} \geq 0.98$	14	24±3
$E_{20}\ P_T^{miss} \geq 1\,\mathrm{GeV}/c$	12	16±3
$P_{tt} \leq 4\,\mathrm{GeV}/c$	7	9.7±2
$\cos(acop) \geq -0.98$	3	3.5±1
$\mathcal{P}_{comb} \geq$-1	1	2.3±0.8

Table 4: Fourth step of the event selection for two-body sbottom decays in the degenerate mass case. The variables are explained in the caption of Table 1 Table 2 and Table 3. DLA stands for discriminating linear analysis.

Squark	Data	MC
$\tilde{\mathrm{t}}$	8	9.3±1.2
$\tilde{\mathrm{b}}$	3	4.4±0.9

Table 5: Number of candidates and expected background in the search for two-body decays of stop and sbottom when performing the "or" of both analyses in the generate and non degenerate mass case.

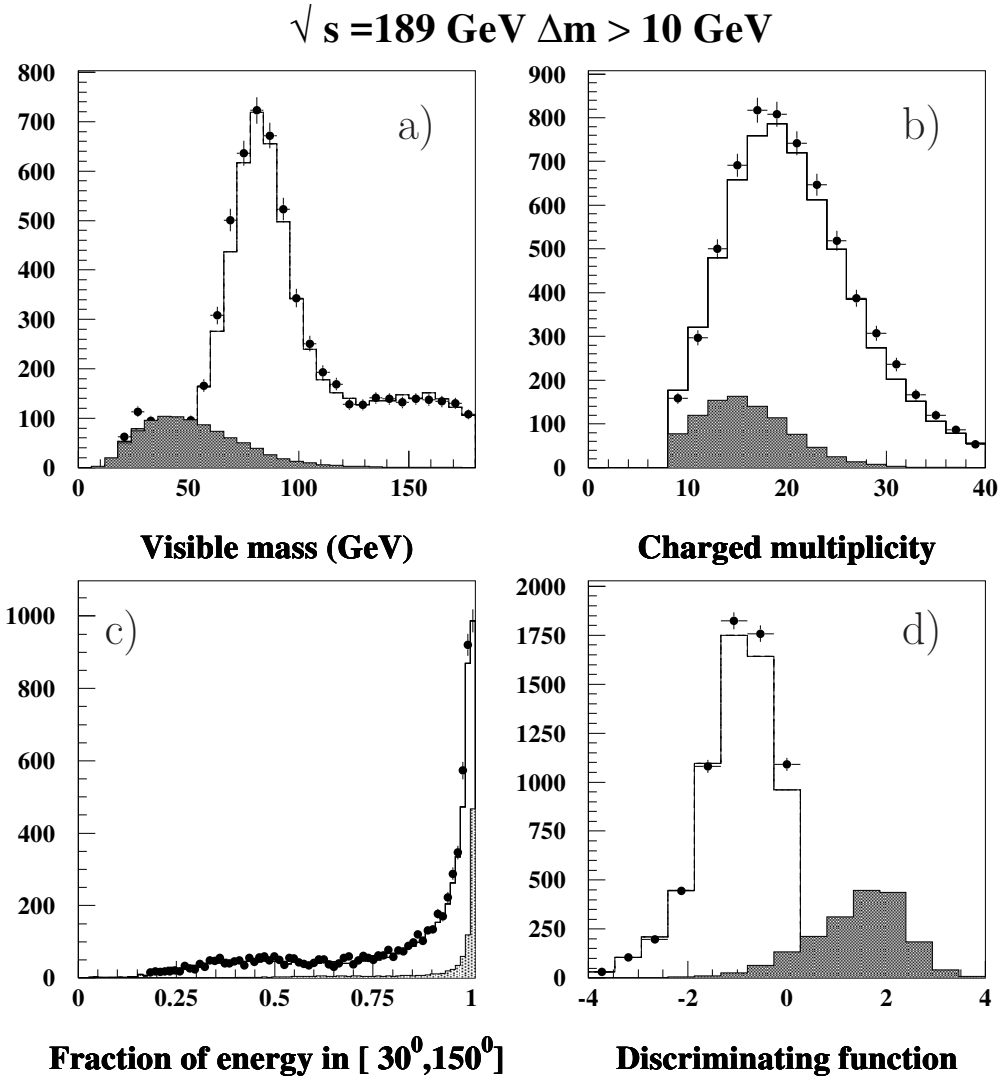

Figure 1: a) the visible mass, b) the charged multiplicity, c) the fraction of the energy in the polar angle interval $[30^o, 150^o]$ and d) the discriminating function against the $Z\gamma$ background (as described in the text) for the non degenerate mass case concerning both stop and sbottom analysis. The dark areas show the stop signal (not normalized to the luminosity).

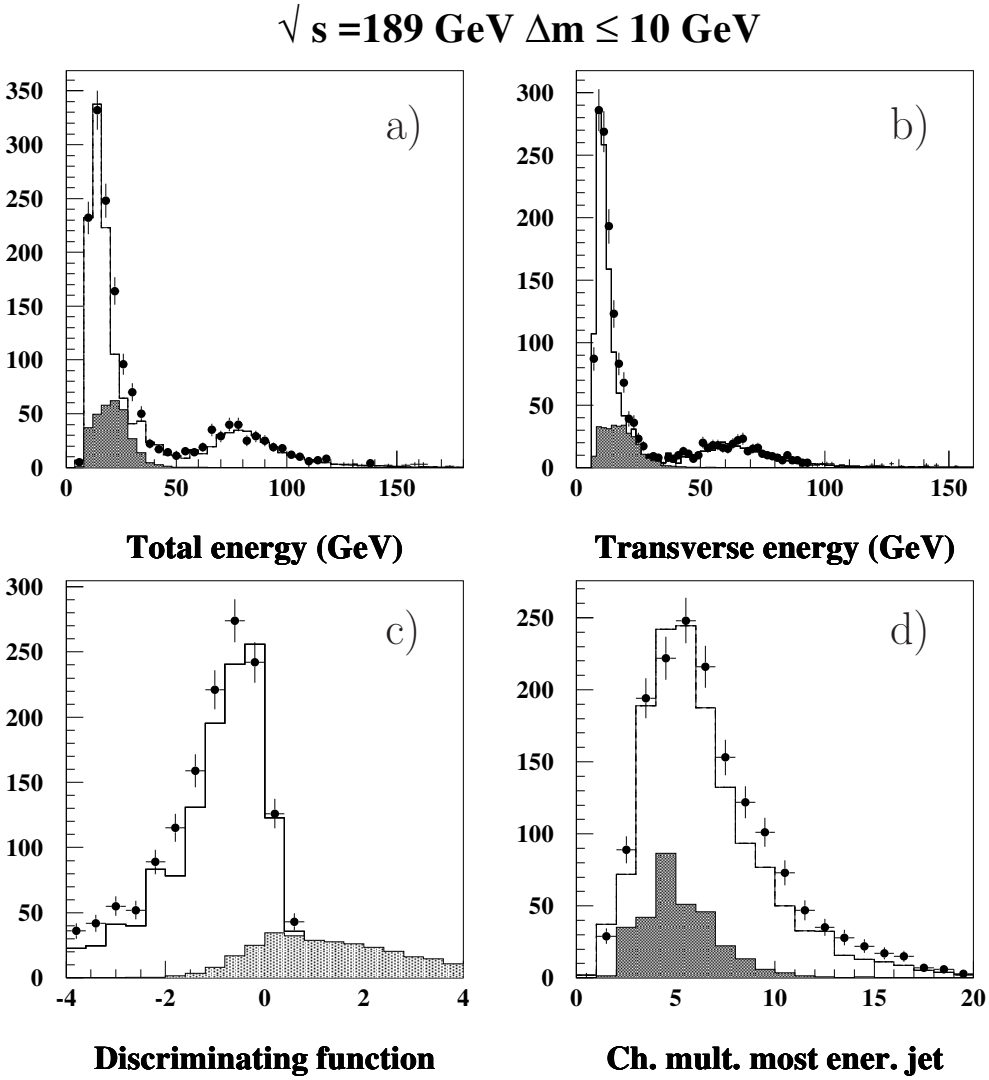

Figure 2: a) the total energy, b) the transverse energy, c) the discriminating function (as described in the text) and d) the charged multiplicity of the leading jet for the degenerate mass case of the stop analysis. The dark areas show the stop signal (not normalized to the luminosity).

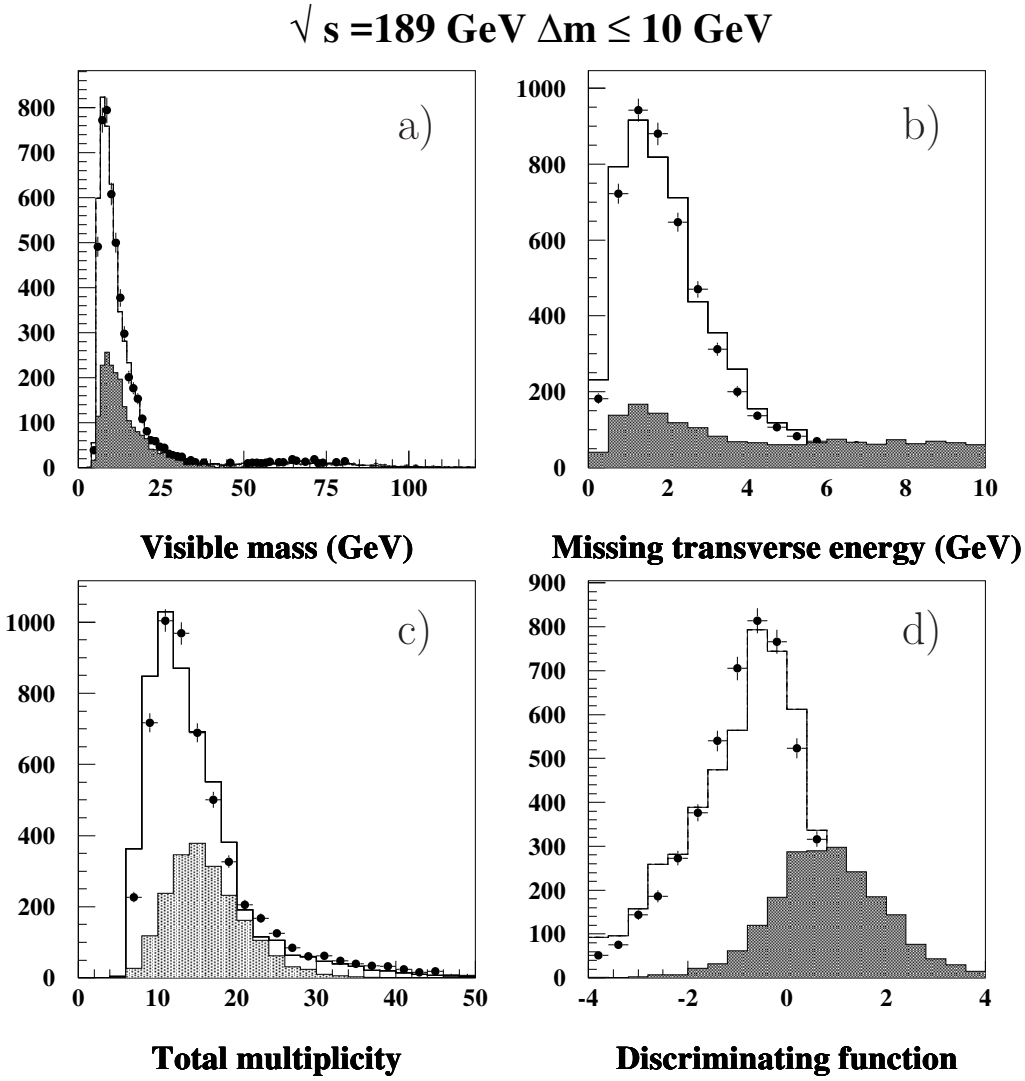

Figure 3: a) the visible mass, b) the missing transverse energy, c) the total multiplicity and d) the discriminating function (as described in the text) for the degenerate mass case of the sbottom analysis. The dark areas show the stop signal (not normalized to the luminosity).

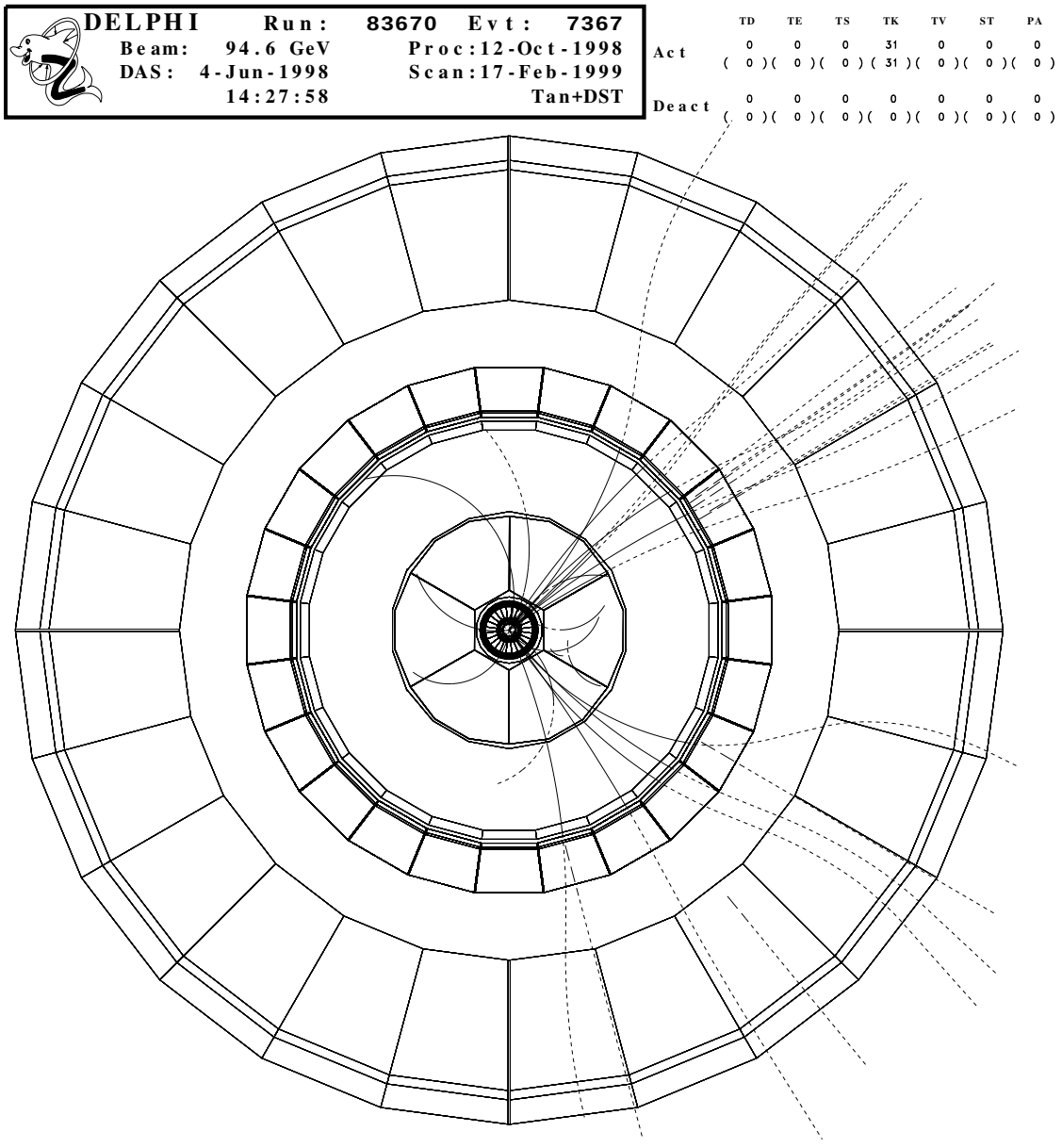

Figure 4: View of one candidate from the non-degenerate mass case in the transverse plane. The corresponding total energy is 57.3 GeV, a charge multiplicity found to be 27, a total visible mass of 43.3 GeV and with the polar angle of the missing momentum at 74.8 degrees and of the two jets at 86.5 degrees and 125 degrees respectively.

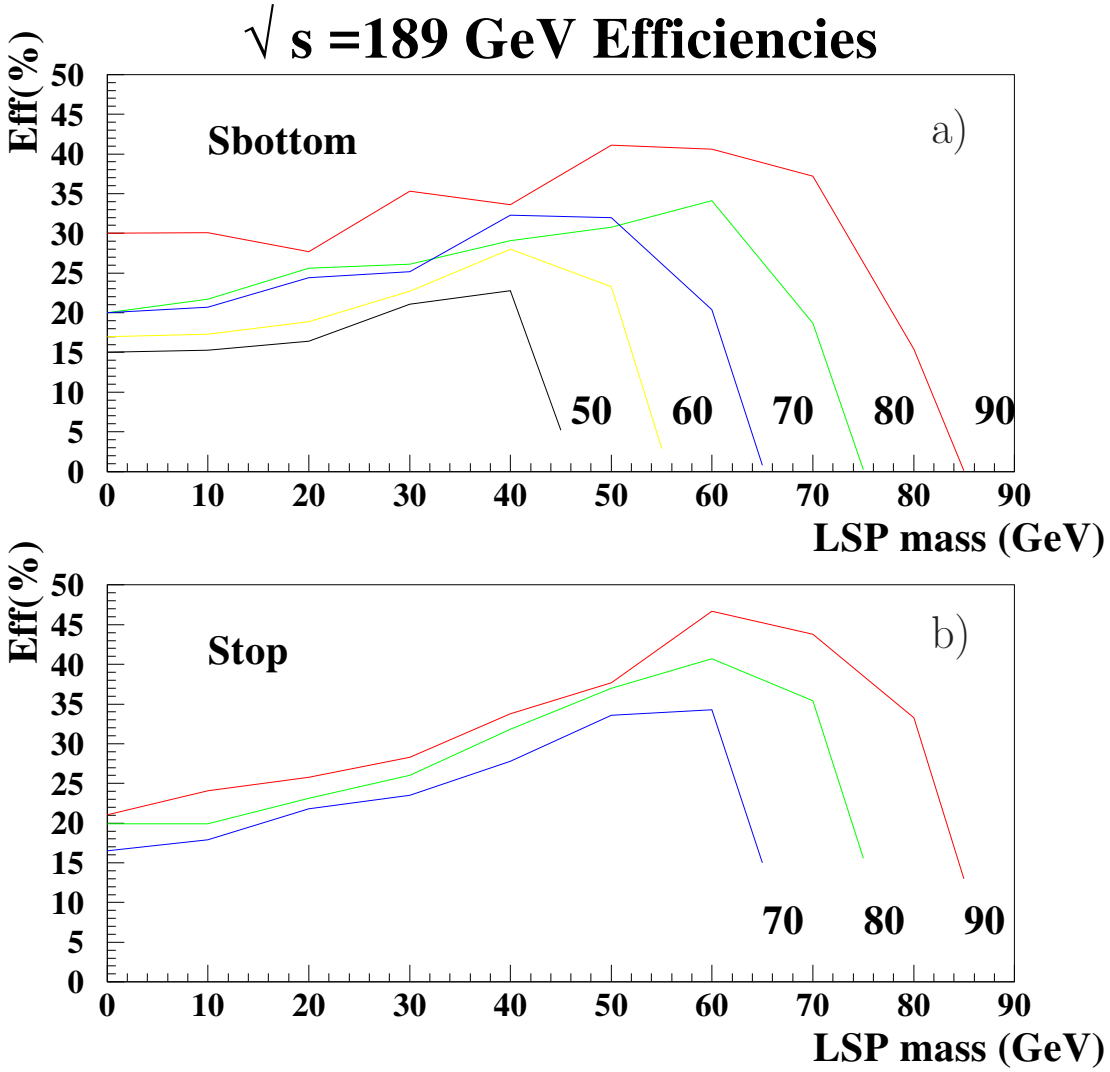

Figure 5: Efficiencies for the sbottom a) and stop b) selection in the search for two-body decays as function of the LSP mass for various sbottom and stop masses. The sbottom and stop masses are indicated on the plots in units of GeV/c^2.

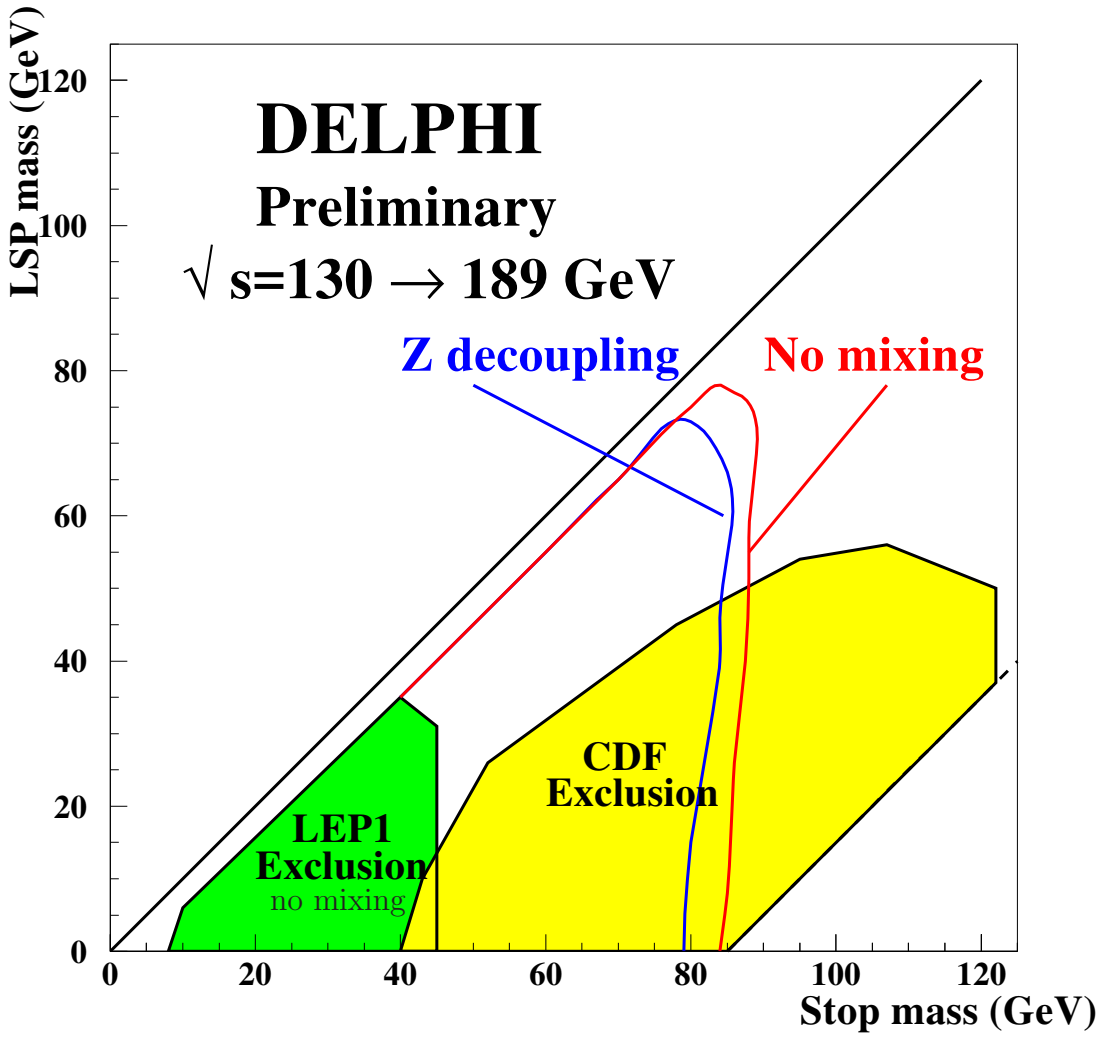

Figure 6: Exclusion domains at 95 % confidence level in the ($\tilde{t}$,$\tilde{\chi}_1^o$) mass plane assuming 100 % branching ratio into c$\tilde{\chi}_1^o$ for pure left-handed state ($\theta = 0$ rad) and for the minimum cross-section ($\theta = 0.98$ rad). The limits are obtained combining data at $\sqrt{s}$ = 161, 172, 183 and 189 GeV. The shaded area have been excluded by LEP1 [22] and CDF [23].

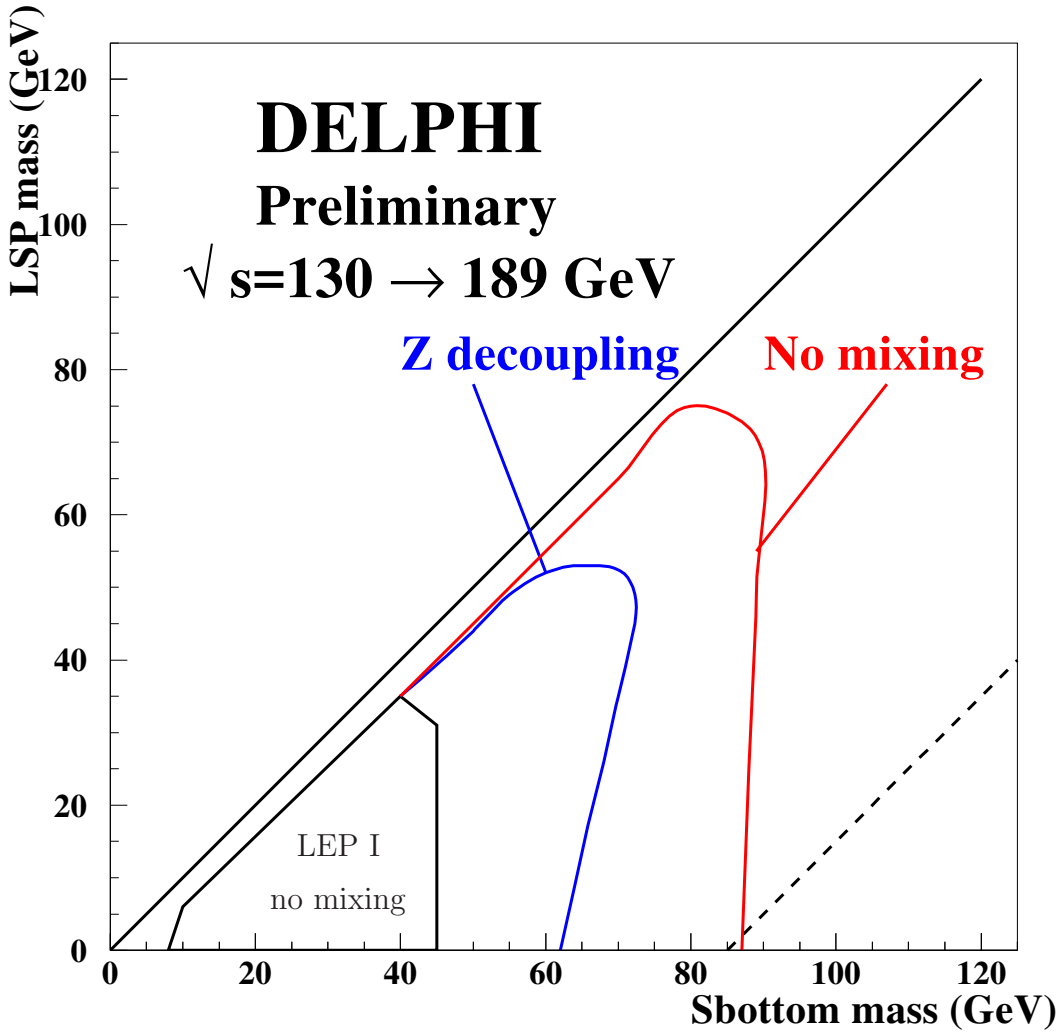

Figure 7: Exclusion domains at 95 % confidence level in the ($\tilde{b}$,$\tilde{\chi}_1^o$) mass plane assuming 100 % branching ratio into b$\tilde{\chi}_1^o$ for pure left-handed state ($\theta = 0$ rad) and for the minimum cross-section ($\theta = 1.17$ rad). The limits are obtained combining data at $\sqrt{s}$ = 130 - 189 GeV.